JOURNAL OF MATERIALS SCIENCE 11 (1976) 215–223

The formation, structure and crystallization of non-crystalline nickel produced by splat-quenching

H. A. DAVIES, J. B. HULL*
Department of Metallurgy, University of Sheffield, St. George's Square, Sheffield, UK

A non-crystalline phase has been formed in electron-transparent (0.1 to 0.5 μm thick) areas of splat-quenched foils of nickel. The positions in diffraction co-ordinates of the first two peaks and of a shoulder on the high-angle side of the second peak of the electron diffraction pattern agree closely with those for non-crystalline vapour-deposited Ni. The presence of the shoulder suggests that the structure is similar to that of dense random packed hard spheres, i.e. that it is amorphous rather than microcrystalline. The crystallization behaviour of the glassy phase studied *in situ* in 1 MV electron microscope also supports this view. The crystallization temperature of about 150° C is unexpectedly high and suggests that stabilization by impurities (possibly up to 0.7 wt %) was occurring. The critical cooling rate for the formation of the glassy phase has been estimated from theories of homogeneous nucleation, crystal growth and transformation kinetics to be $\sim 10^{10}$ K sec^{-1} which is in satisfactory agreement with experimentally derived estimates of the maximum cooling rate in electron-transparent areas of foils.

1. Introduction

Since the original gun technique of splat-quenching was introduced [1] a large number of metallic alloys has been quenched into a non-crystalline form in foil thicknesses ranging from 10 μm to about 2 mm. Generally, these alloys have been based on noble or transition metals and had compositions at or near to deep, low-melting eutectics, where the liquid viscosity is high, two conditions that favour glass formation. However, by quenching in an inert atmosphere and careful electron microscopic examination, amorphous phases have been observed in the thinnest, electron-transparent areas around the edges of quenched foils of a number of aluminium-based alloys, some consisting only of metallic components, where the cooling rate was estimated to be in excess of 10^9 K sec^{-1} [2–4].

Subsequently, elemental semi-metallic amorphous phases, germanium and tellurium [3] were also produced in thin sections by this method and this raised speculation as to whether any material could be liquid-quenched to a glass providing the cooling rate is high enough and that the final temperature is sufficiently low to avoid immediate crystallization. Although no metallic elements had been splat-quenched to the glassy state, a number, including several cubic metals such as Co, Ni, Pd and Fe, had been produced as amorphous films by vapour-deposition techniques [5-8]. In some cases, amorphous Ni films, stabilized by impurities, were reported as being stable at room temperature [5-6]. Also, Ni has a particularly high viscosity and temperature dependence of viscosity above its melting temperature [9] and is a major component of several alloys that have been splat-quenched into the glassy state [10]. Hence, it was considered possible that Ni could be liquid-quenched to the glassy state.

This paper gives a more complete account of the results of an electron microscopic and diffraction study of the structure and crystallization behaviour of a glassy splat-quenched Ni phase,

*Present address: Department of Metallurgy, Sheffield Polytechnic, Pond Street, Sheffield, UK.

briefly described previously [11]. The kinetics of formation of the phase are also considered and the theoretically derived critical cooling rate compared with experimentally estimated values for the electron-transparent areas of quenched foils.

2. Experimental procedure

Small portions (~50 mg) of nickel (99.998% pure) were splat-quenched from a temperature of 1550° C on to a water-cooled curved copper surface using a shock-tube quenching device, similar in design to that developed by Duwez and Willens [12]. In order to minimize oxidation of the nickel, a continuous flow of argon gas was maintained along the low pressure section of the shock tube and through the crucible orifice, above which the nickel droplet was held, prior to quenching. A blanket of argon was also maintained in the region between the crucible and the substrate in order to limit surface oxidation of the atomized particles and thus promote efficient spreading of the droplets and good thermal contact with the substrate. Heating was effected by means of an r.f. coil, the boron nitride crucible being surrounded by a snug-fitting jacket of graphite which acted as a susceptor and reduced thermal gradients around the nickel droplet. The crucible orifice length: diameter ratio was made as large as possible (>6) to minimize the mean atomized particle diameter [13] which gave shorter heat transfer paths and hence higher cooling rates.

The quenched foils were essentially porous composites of individually solidified droplets. Preliminary structural examination of segments of the as-quenched foils were performed in a 100 kV electron microscope, substantial areas around the foil edges being transparent to 100 keV electrons. However, all quantitative diffraction and micrographic investigations were made with an AEI EM7 1000 kV microscope which gave a six-fold increase in penetrable thickness and/or greater intensity with less inelastic background scattering in diffraction work. A temperature-calibrated heating stage was used for *in situ* studies of crystallization of the glassy phase.

3. Results

Some of the quenched droplets at the edges of the nickel foil fragments, which were transparent to 100 keV electrons and estimated to have thicknesses of about 0.1 μm, showed no micrographic features even at magnifcations of over × 100 000. Moreover, many of the droplets which were opaque to 100 keV electrons but transparent to 1 MeV electrons and estimated to be up to 0.5 μm thick, were also structureless (Fig. 1a). The diffraction patterns for these areas consisted of diffuse haloes, characteristic of non-crystalline materials (Fig. 1b), two haloes being clearly visible but a third, at a higher angle, was only just resolvable on the photographic negative with the naked eye. This is the first reported instance of a metallic element formed as a glass by continuous cooling from the liquid.

The positions K_{pi} of the two main peaks in the intensity distribution and that of a shoulder

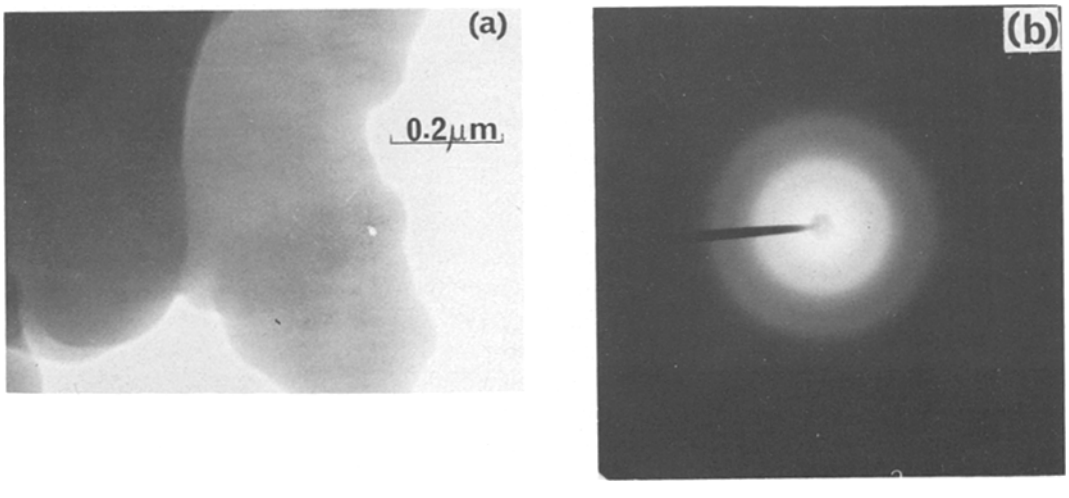

Figure 1 (a) 1000 keV transmission electron micrograph of an amorphous area at the edge of a splat-quenched foil of nickel. (b) Selected-area diffraction pattern of amorphous area.

TABLE I Mean diffraction peak positions for non-crystalline splat-quenched and vapour-deposited Ni and for liquid Ni

	$K = 4\pi \sin\theta/\lambda (\text{Å}^{-1})$			
	Peak 1	Peak 2	Peak 2 shoulder	Peak 3
Splat-quenched Ni (ED)	3.11 ± 0.07	5.48 ± 0.1	5.96 ± 0.1	
Vapour-quenched Ni (ED) [32]	3.18	5.40	5.91	7.95
Liquid Ni (ND) [14]	3.10	5.85		8.10

Notes: ED. electron diffraction; ND, neutron diffraction.

on the high-angle side of the second peak were determined from microdensitometer traces of the patterns; these are given in Table I, expressed as the diffraction co-ordinate $s = 4\pi \sin\theta/\lambda$ (Å^{-1}) where θ is the diffraction angle and λ the wavelength of the electron radiation. (The camera constant was established independently using samples of fine polycrystalline aluminium.) The corresponding values of K_{pi} for liquid nickel, determined by neutron diffraction [14], and for amorphous vapour-deposited thin films of nickel, determined by electron diffraction [7] are also presented. The first peak positions for all three phases are in close agreement and the positions of the second maximum and its high-angle shoulder are also in good agreement for the splat-quenched and vapour-deposited phases (the second peak for the molten phase shows no shoulder, possibly because it is smeared out by the additional thermal broadening at the high temperatures, and the resultant maximum lies at an intermediate value of s, at 5.8 Å^{-1}).

On heating the splat-quenched glassy phase, crystallization began at 425 ± 5 K, proceeding

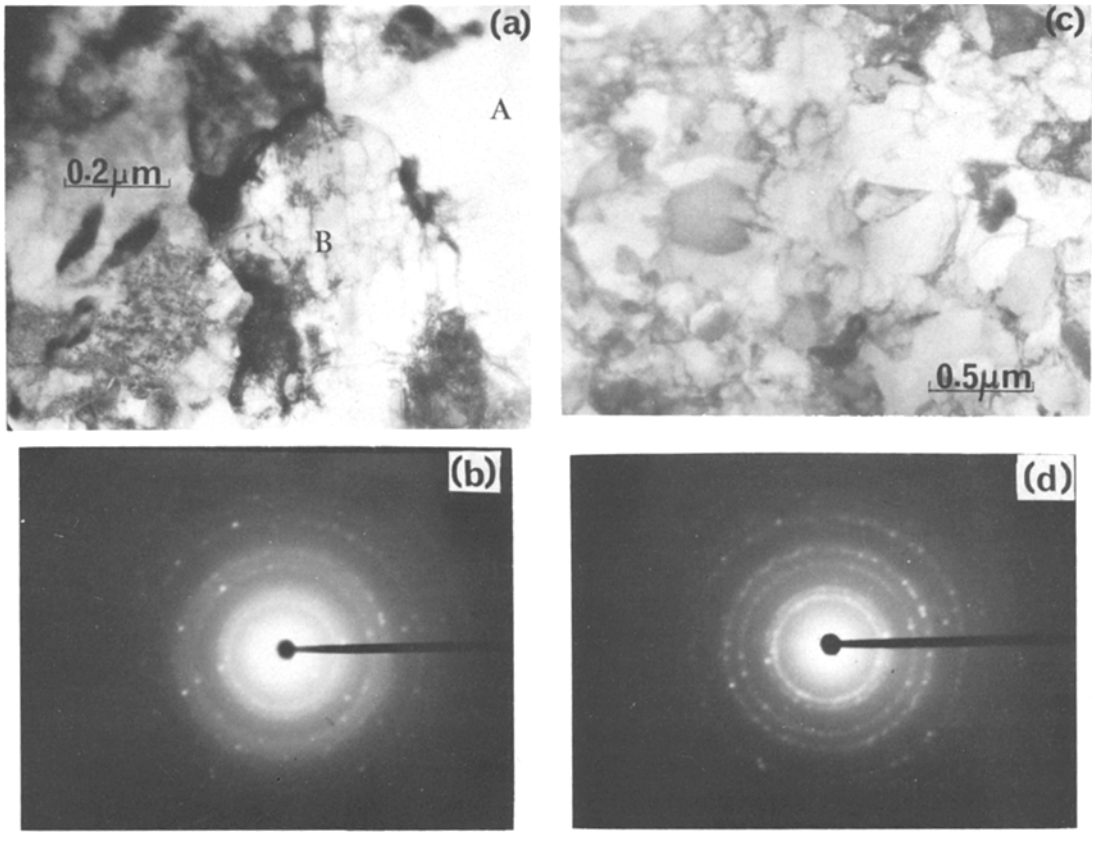

Figure 2 (a) Region near an amorphous/crystal boundary with crystallization largely arrested by rapid cooling after partial crystallization by heating (1000 keV). A – amorphous B – crystalline – not sharply defined because process not completely arrested; also evidence of straining resulting from the crystallisation. (b) Selected-area diffraction pattern of boundary region. Spotty diffraction rings of the crystalline phase are superimposed on the haloes of the noncrystalline phase. (c) Micrograph of the area shown in (a) after complete crystallization due to heating. (d) Selected-area diffraction pattern of the fully crystallized structure shown in (c).

rapidly by a nucleation and growth process. Owing to the design of the heating stage, however, the specimen temperature was not uniform, the heat being transferred to the specimen largely along those grid bars with which it was in intimate thermal contact. Hence, fronts behind which crystallization began, were seen to move away from these regions of grid contact. This could sometimes be arrested at various stages (though good control was difficult) by cooling as rapidly as possible to a temperature well below 425 K. Micrographs and some corresponding selected-area diffraction patterns for initially glassy areas are shown in Fig. 2a to d during two stages of crystallization. Spotty diffraction rings of the crystalline phase, indexed as f c c Ni, appeared superimposed on the haloes of the glassy phase. The ring intensities increased and the halo intensities decreased as the transformation proceeded, without any apparent decrease in the breadth of the latter. Behind the moving crystallization fronts, arrays of dislocations moved rapidly under the action of the thermal stresses.

4. Discussion

4.1. Structure

The close similarity between the diffraction peak positions of the non-crystalline splat-quenched and vapour-deposited phases strongly suggests that they have similar structures. A radial distribution analysis could not be meaningfully performed in the present case because of the relatively large thickness of the glassy area and the consequent very large proportion of scattered radiation.

It has been shown [15] that a characteristic of model dense random packed hard sphere (drphs) structures is a shoulder on the high-angle side of the second peak of the pair distribution function $W(r)$. The $W(r)$ functions of many non-crystalline metals and alloys prepared by splat-quenching, vapour-condensation techniques or by electroless deposition, derived by Fourier inversion of experimental coherently diffracted intensity distributions $I(s)$, show this feature [16, 17]. On this basis, it has been concluded that non-crystalline vapour-deposited Ni has a structure very similar to that of drphs but differing in detail from it [7]. Many of the non-crystalline metallic phases believed to have drphs structures, including Ni, have a high-angle shoulder on the second peak of $I(s)$. By analogy with the vapour-deposited Ni, we can tentatively conclude that the splat-quenched non-crystalline Ni also has a structure approximating to drphs.

Further evidence that the glassy phase has an amorphous rather than microcrystalline structure is gained from the crystallization studies. Crystallization occurred rapidly by a nucleation and growth process, with the diffraction rings of the crystalline phase superimposed on the broad haloes of the untransformed phase, without apparent sharpening of these haloes as crystallization proceeded, despite the fact that the latter phase has been heated above the transformation temperature. In contrast, a structure consisting initially of microcrystallites would be expected, on heating, to undergo rather slower crystallite coarsening over a wider temperature range, giving continuous sharpening of the broad haloes.

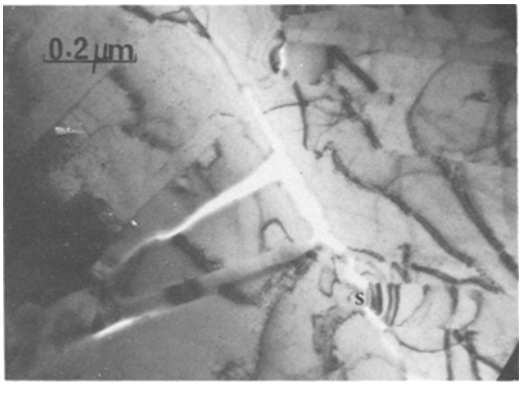

Figure 3 Grain-boundary separation at a triple point after crystallization of an initially amorphous area, probably resulting from the contraction associated with the glass/crystal transformation, advancing from two or more directions.

A fully crystallized region is shown in Fig. 3 where grain-boundary separation of about 30nm has occurred at a triple point, probably as a result of the volume contraction associated with the glass/crystal transformation; the process of separation was observed as crystallization proceeded. A high density of bend contours is associated with one narrow element of material (marked s) still bridging two grains.

4.2. Stability

The crystallization temperature for the glassy Ni was remarkably high at 425 K, the process occurring rapidly over a narrow temperature range. Bosnell [6] and Fujime [5] have both reported that non-crystalline vapour deposited Ni was

stable when heated at room temperature although the actual T_c was not reported in either case. Tamura and Endo [31] found a very high T_c of 530 K for similar films although again, the impurity concentration was not given. More recently, Bennett and Wright [8] have determined the effect of gaseous impurity content on the stability of the non-crystalline phase; they concluded that for 0.07% of gaseous impurities the structure was probably microcrystalline with recrystallization extending over the range 230 to 300 K whereas for 0.75% of gaseous impurities the structure is amorphous with rapid crystallization occurring at a much lower temperature – below 100 K. Grundy *et al.* [18] consider that Ni films containing about 1% gaseous impurity can be vapour-condensed at 77 K in the amorphous state and show that such films crystallize at about 200 K.

Although the composition of the initial solid Ni is known in the present case (20 ppm metallic impurities, < 100 ppm [O]), the gaseous impurity content of the final splat, and particularly the oxygen and carbon contents in the glassy areas is much more difficult to establish. Oxygen may have dissolved in the initial droplet from slight atmospheric contamination of the argon flow in the low-pressure part of the shock-tube or in the atomized droplets from contamination of the blanket gas, although the latter possibility is much less likely since the time available for solution of gas during the droplet propulsion stage is < 1 msec (the maximum solubility of [O] in liquid Ni at the pre-quenching temperature of 1725 K is about 2 at.% whereas that for [N] is negligibly small [19]). There is also a slight possibility that carbon from the graphite crucible was also a contaminant. Electron-probe microanalyses performed with a Cambridge Microscan V on thick regions of splat as close to the edges as was practicable indicated concentrations of [O] and C below the detection limits [20] of 0.5% and 0.2%, respectively. This suggests only that the non-metallic impurity content of the glassy phase was less than 0.7 wt%, or about 2.5 at.%.

The magnitude of T_c for this splat-quenched glassy Ni is probably consistent with those for the vapour deposited films of, in general, apparently lower impurity contents. It is noted, however, that the results for condensed films are not themselves wholly consistent with each other [33]; it is possible that metallic impurities such as tungsten and molybdenum, from evaporating filaments, in some cases stabilized the films and that factors other than impurity content, such as substrate temperature and rate of condensation might influence their stabilities by giving very slight deficits in packing density or, alternatively, microvoids, for which there is some evidence in condensed Ge films [21], for instance. There is, on the other hand, no clear evidence that the splat-quenched glassy Ni has a significantly lower mean interatomic distance than that of the amorphous vapour deposited Ni. In summary, although it is inevitable that some impurity stabilization occurred in the present glassy phase, it is not possible from the present results to establish fully the extent and effect of this. Experiments in which the impurity, and particularly oxygen, concentration of the quenching environment was varied in a controlled way, coupled with corresponding cooling rate measurements would be required for this.

4.3. Kinetics of formation

It is of interest to speculate on the glass transition temperature T_g for liquid nickel and thus on the critical cooling rate required for the formation of impurities, T_c would be above T_g, as is T_c as a lowest possible limit of T_g since it is highly improbable that, in a nominally pure, close-packed phase, stabilized by a low concentration of impurities, T_c would be above T_g, as is observed in many glassy alloys. T_c for pure metals is very sensitive to the presence of impurities since these tend to segregate at the crystal/glass boundaries. As a result, the crystallization process, which in very pure, close-packed glassy systems involves rearrangement by atomic jumps of only fractions of the atomic diameter across the interface, may require more extensive interfacial rearrangements with an appreciable activation energy. On the other hand, T_g would be relatively insensitive to impurity levels of the order of 1% since the process of relatively rapid atomic drift which characterises temperatures above T_g requires cooperative motion of large numbers of atoms.

We have recently proposed a speculative viscosity–temperature curve for Ni in the temperature range between the melting point T_m and T_g [22]. We derived from this, using established theories of homogeneous nucleation, crystal growth and the Johnson–Mehl–Avrami treatment of trans-

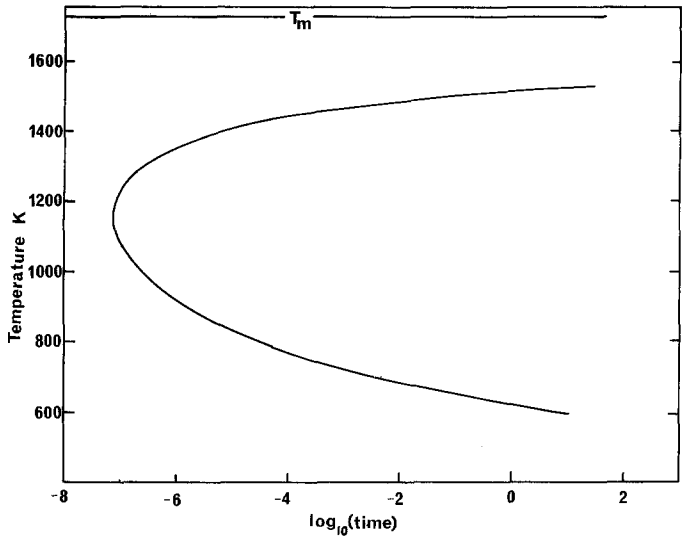

Figure 4 Time–transformation curve representing the time required for an arbitrarily very small fraction of crystallization (10^{-6}) as a function of temperature below the normal freezing point for pure liquid nickel.

formation kinetics, a time–temperature–transformation (T-T-T) curve expressing the time t for a barely detectable fraction X of crystallization (taken to be 10^{-6}) as a function of temperature T [22, 23]. This is shown in Fig. 4. If the time and temperature corresponding to the nose of this curve are τ_N and T_N, respectively, the critical cooling rate R_c required to avoid the crystal fraction 10^{-6} is then given approximately by $[(T_m - T_N)/\tau_N]$ i.e. $\sim 5 \times 10^9 \text{K sec}^{-1}$. R_c is relatively insensitive to the choice of X since $t \propto X^{1/4}$; thus, setting $X = 10^{-10}$, which is a hypothetically small fraction, only increases R_c by one order of magnitude. (In the field of view shown on a photograph such as Fig. 1a at $\times$ 100 000, $X = 10^{-6}$ would represent, for example, one crystal of diameter $\sim$6 nm or 27 crystals of diameter $\sim$2 nm). The maximum uncertainty in R_c arising in particular from uncertainties in the assumed viscosity and in the application of homogeneous nucleation theory is estimated to be $\pm$ two orders of magnitude but with a more probable uncertainty of $\pm 1\frac{1}{2}$ orders of magnitude. (The maximum cooling rate in a thickness of 0.1 μm of iron, which has a similar thermal conductivity to nickel, assuming perfect thermal contact with the substrate has been calculated to be 9×10^{11} K sec^{-1}) [24].

Direct experimental estimates have been made of the cooling rates obtaining in splat-quenching by this gun technique, by means of a thermocouple coupled to an oscilloscope [25] and by using high-speed photography [26]. They both give a value of 10^6 K sec^{-1} but this is a lower limit which, in the former case at least, pertains only to the thick regions of splat. To estimate experimentally the cooling rate in the electron-transparent regions we have used two independent microstructural methods, one involving the determination of interlamellar spacing in a eutectic Al–Cu alloy [27] and the other the measurement of secondary dendrite-arm spacings in a number of Al-based alloys [28]. Using a 100 kV electron microscope, clearly resolvable lamellae were observed in the Al–Cu alloy down to a spacing of $\sim$10 nm (although lamellae with smaller spacings down to 7 nm, but generally illdefined, were also observed in 100 keV transparent regions); this corresponds to a cooling rate of $\sim 3 \times 10^9$ K sec^{-1} in a thickness of 0.15 μm [4]. The minimum secondary dendrite arm spacings in both Al–6% Pd and Al–11% Si were of the order of 30 nm, which again corresponds to a cooling rate of 3×10^9 K sec^{-1}.

Since amorphous phases were also observed in electron-transparent areas of the quenched Al–Cu, Al–Si and Al–Pd alloys we must presume that they probably resulted from still higher cooling rates – of the order of 10^{10} K sec^{-1}. Moreover, the noncrystalline Al–Cu phase was also observed in microscope foils which were prepared by chemically thinning some of the thicker regions of splat. This implies that some individual droplets in the atomized spray were cooling to below the T_g of the alloy before succeeding droplets arrived to be quenched on top of them. The cooling rate required for this, based on an idealized model of the liquid spray, is again estimated to be

of the order of 10^{10} K sec^{-1} (see Appendix).

Hence, although each of the experimental estimates is subject to considerable uncertainty the agreement between the results suggests that the theoretical estimate of R_c is within an order of magnitude correct and that the assumptions involved in its derivation are broadly correct. In particular, the assumption of homogeneous nucleation may be valid because the electron-transparent areas are formed by the spreading of the smallest droplets in the droplet size distribution of the atomized spray, largely those less than 1 μm in diameter [25]. Many of these are likely, statistically, to be free of heterogeneous nuclei, particularly if the impurity content is low [29]. Where the thermal contact with the substrate during spreading is sufficiently good, such droplets would be expected to solidify completely to a glassy structure. Hence, the objection that has been raised that an elemental close-packed glass that was formed only in the thin areas should immediately crystallize through crystal growth from adjacent crystalline thicker areas [30] would not necessarily be valid since the glassy phase exists in individually solidified droplets at the edges of the foil, many of which need not be in intimate atomic contact with adjacent crystalline droplets.

Although the high temperature section of the T-T-T curve theoretically continues to rise extremely slowly up to T_m, it gives an indication of the minimum temperature to which molten Ni could be undercooled, in practice, assuming homogeneous nucleation only. Turnbull [34] gives the homogeneous nucleation frequency I_v at maximum undercooling as $10^{6(\pm 1)}$. From the variation of I_v with temperature for Ni given in Fig. 5, this gives an undercooling of about 0.17 T_m in this case, which compares fairly well with the value of 0.185 T_m observed experimentally by Turnbull [29]. The T-T-T curve clearly demonstrates also why the undercooling is essentialy independent of cooling rate (until the latter becomes sufficiently high that the cooling curves intercepts the T-T-T curve near to its nose and eventually by-passes the nose).

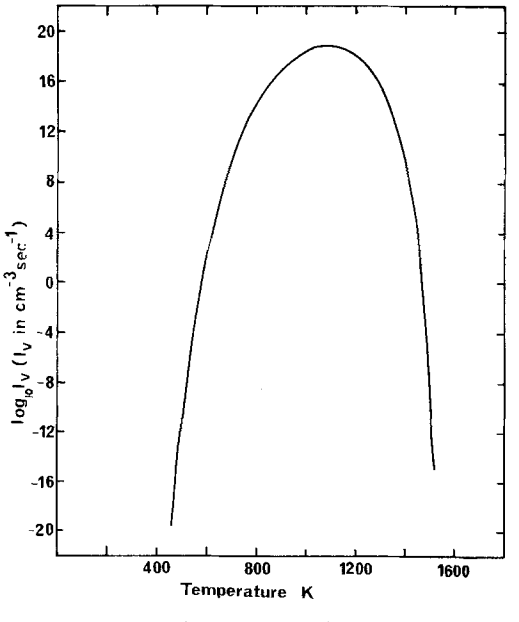

Figure 5 Calculated variation with temperature of the nucleation frequency.

5. Conclusions

(1) Non-crystalline nickel has been produced by the gun technique of splat-quenching in the thinnest regions up to 0.5 μm thick at the edges of foils. This is the first reported instance of a close-packed elemental glass formed by liquid-quenching.

(2) The diffraction peak positions are very similar to those for non-crystalline vapour-deposited nickel and for liquid nickel. In particular, the shoulder which appears on the high-angle side of the second peak suggests that the structure of the liquid-quenched glass is that of dense random-packed hard spheres, i.e. amorphous rather than microcrystalline. This is also supported by the crystallization studies.

(3) The glassy phase is very probably stabilized by impurities but it is not possible from the present results to establish the degree of stabilization.

(4) The critical cooling rate required for the formation of the glassy phase has been estimated theoretically to be of the order of 10^{10} K sec^{-1} This is in satisfactory agreement with estimates of the maximum cooling rate obtaining in this quenching method, derived experimentally from microstructural observations on quenched alloys.

Appendix. Calculation of the critical cooling rate required for the formation of a glassy Al–17.3% Cu phase within thick regions of splat

Non-crystalline Al–17.3% Cu was observed in electron microscope foils that had been chemically thinned from the thicker areas of splat-

quenched foils. This implies that some individual droplets in the atomized liquid spray were cooling to below T_g and T_c for the phase before succeeding droplets arrived to be quenched on top of them. We can estimate the cooling rate that would be required for this to occur.

Consider the initial molten droplet of alloy having volume V_s. This is then propelled through the crucible orifice of diameter d_0 and atomized by the shock wave (see Fig. 6).

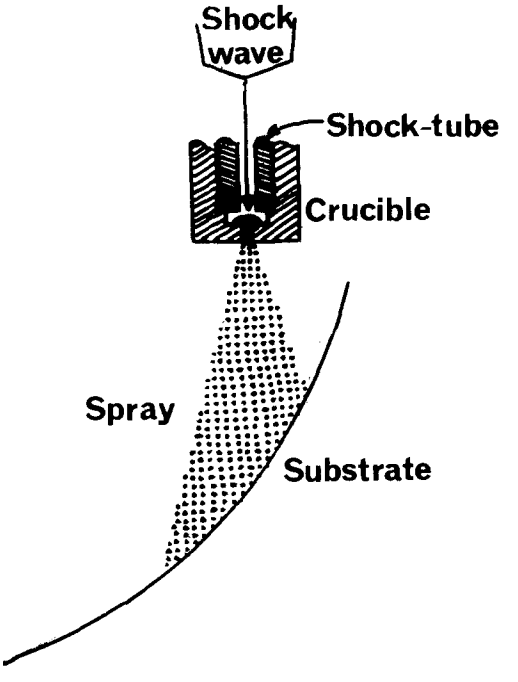

Figure 6 Schematic representation of the propulsion of the molten droplet through the crucible orifice and the subsequent atomisation. An idealized simple cubic distribution of atomized droplets is assumed.

$\therefore$ "length" of molten specimen after passing through orifice $= V_s \Big/ \frac{\pi d_0^2}{4} = \frac{4V_s}{\pi d_0^2}$

Let A = cross-sectional area of spray at substrate

$\therefore$ total volume taken up by spray at substrate

$$= \frac{4AV_s}{\pi d_0^2}. \quad (1)$$

Let the mean particle diameter $= d_p$

$\therefore$ total number of particles in spray $\cong V_s \frac{\pi d_p^3}{6}$. (2)

Average number of particles/unit volume at substrate $= 3d_0^2/(2d_p^3 A)$ (from Equations 1 and 2). Let the velocity of the atomized particles $= v$. Assume the particles are distributed as a simple cubic lattic with direction of motion parallel to ⟨1 1 1⟩.

$\therefore$ average vertical distance between particles

$$= \sqrt{3}\left(\frac{3d_0^2}{2d_p^3 A}\right)^{-1/3},$$

$\therefore$ average time between superimposed quenching events $t_a = \frac{\sqrt{3}d_p}{v}\left(\frac{2A}{3d_0^2}\right)^{1/3}$.

Let the interval between initial temperature and glass transition temperature $= \Delta T_g$. The droplet must cool through ΔT_g before the succeeding droplet arrives on top of it.

$\therefore$ rate of cooling τ should be $\gtrsim \frac{\Delta T_g}{t_a}$

$$\gtrsim \frac{\Delta T_g}{\sqrt{3}d_p}\left(\frac{3d_0^2}{2A}\right)^{1/3} \quad (3)$$

v has been found to be $\sim 300\,\mathrm{m\,sec^{-1}}$ [25]. The mean particle diameter d_p for this shock-tube quenching technique, given by an experimentally determined particle size distribution curve for pure Al [25], is $\sim 3\,\mu$m. (Particles having $d_p < 1\,\mu$m were not, however, counted in that study.)

T_c for the glassy eutectic Al–Cu phase was found to be ~ 525 K. Assuming as an approximation that $T_g = T_c$ and since the initial temperature prior to quenching in that case was ~ 1025 K, $\Delta T_g = 500$ K.

$\therefore$ from Equation 3 $\quad \tau \gtrsim 1.2 \times 10^{10}\,\mathrm{K\,sec^{-1}}$.

Acknowledgements

The authors wish to thank Drs Brian Lewis and David Warrington for helpful comments and discussions and Professors B.B. Argent and G.W. Greenwood for providing laboratory facilities. They also gratefully acknowledge the financial support of the Science Research Council and the use of the SRC/BSC 1000 kV electron microscope facility at Swinden Research Laboratories.

References

1. W. KLEMENT JR. and P. DUWEZ, *Nature* **187** (1960) 869.

2. P. RAMACHANDRARAO, M. LARIDJANI and R.W. CAHN, *Z. Metallk.* **63** (1972) 43.
3. H. A. DAVIES and J. B. HULL, *J. Mater. Sci.* **9** (1974) 707.
4. J. B. HULL and H. A. DAVIES, Presented at the International Conference on Rapidly Quenched Alloys, November 1975.
5. S. FUJIME, *Jap. J. Appl. Phys.* **6** (1967) 305.
6. J. R. BOSNELL, *Thin Solid Films* **3** (1969) 233.
7. L. B. DAVIES and P. J. GRUNDY, *Phys. Stat. Sol.* **A8** (1971) 189.
8. M. R. BENNETT and J. G. WRIGHT, *ibid.* **A13** (1972) 135.
9. R. T. BEYER and E. M. RING, "Liquid Metals – Physics and Chemistry" edited by S.Z. Beer (Dekker, New York, 1972) p. 431.
10. H. JONES and C. SURYANARAYANA, *J. Mater. Sci.* **8** (1973) 705.
11. H. A. DAVIES, J. AUCOTE and J. B. HULL, *Nature-Phys. Sci.* **246** (1973) 13.
12. P. DUWEZ and R. H. WILLENS, *Trans. Met. Soc. AIME* **227** (1963) 362.
13. C. H. JANSEN, Ph.D. Thesis, MIT (1971).
14. Y. WASEDA, K. SUZUKI, S. TAMAKI and S. TAKEUCHI, *Phys. Stat. Sol.* **39** (1970) 181.
15. J. L. FINNEY, Ph.D. Thesis, University of London (1968).
16. G. S. CARGILL III, *J. Appl. Phys.* **41** (1970) 12, 2248.
17. B. C. GIESSEN and C. N. J. WAGNER, "Liquid Metals – Physics and Chemistry", edited by S.Z. Beer (Dekker, New York, 1972) p.633.
18. P. J. GRUNDY, S. S. NANDRA and A. ALI, presented at Intermag Conference 1975.
19. M. HANSEN, "Constitution of Binary Alloys" McGraw-Hill, New York, 1958) and R. P. ELLIOTT, 1st Supplement (McGraw-Hill, New York, 1965).
20. C. W. HAWORTH, private communication.
21. T. B. LIGHT, *Phys. Rev. Letters* **22** (1969) 999.
22. H. A. DAVIES, J. AUCOTE and J. B. HULL, *Scripta Met.* **8** (1974) 1179.
23. H. A. DAVIES, *J. Non-Cryst. Solids* **17** (1975) 266
24. R. C. RUHL, *Mat. Sci. Eng.* **1** (1967) 313.
25. P. PREDECKI, A. W. MULLENDORE and N. J. GRANT, *Trans. Met. Soc. AIME* **233** (1965) 1581.
26. P. DUWEZ, "Phase Stability in Metals and Alloys" edited by P. S. Rudman, J. Stringer and R.I. Jaffee (McGraw-Hill, New York, 1967) p.523.
27. M. H. BURDEN and H. JONES, *J. Inst. Metals* **98** (1970) 249.
28. H. MATYJA, B.C. GIESSEN and N. J. GRANT, *ibid*, **96** (1968) 30.
29. D. TURNBULL, *J. Appl. Phys.* **21** (1950) 1022.
30. *Idem. J. Physique, Supplement C-4* (1974) 1.
31. K. TAMURA and H. ENDO, *Phys. Letters* **29A** (1969) 52.
32. L. B. DAVIES and P. J. GRUNDY, private communication.
33. P. K. LEUNG and J. G. WRIGHT, *Phil. Mag.* **30** (1974) 995.
34. D. TURNBULL, *J. Chem. Phys.* **18** (1950) 769.

Received 18 July and accepted 29 July 1975.